Tracking of Time-Varying Mobile Radio Channels—Part II: A Case Study

Lars Lindbom, Anders Ahlén, *Senior Member, IEEE*, Mikael Sternad, *Senior Member, IEEE*, and Magnus Falkenström

Abstract—Low-complexity WLMS adaptation algorithms, of use for channel estimation, have been derived in a companion paper. They are here evaluated on the fast fading radio channels encountered in IS-136 TDMA systems, with the aim of clarifying several issues: How much can channel estimation performance be improved with these tools, as compared to LMS adaptation? When can an improved tracking MSE be expected to result in a meaningful reduction of the bit error rate? Will optimal prediction of future channel estimates significantly improve the equalization? Can one single tracker with fixed gain be used for all encountered Doppler frequencies and SNR's, or must a more elaborate scheme be adopted? These questions are here investigated both analytically and by simulation. An exact analytical expression for the tracking MSE on two-tap FIR channels is presented and utilized. With this tool, the MSE performance and robustness of WLMS algorithms based on different statistical models can be investigated. A simulation study then compares the uncoded bit error rate of detectors, where channel trackers are used in decision directed mode in conjunction with Viterbi algorithms. A Viterbi detector combined with WLMS, based on second order autoregressive fading models possibly combined with integration, provides good performance and robustness at a reasonable complexity.

Index Terms—Adaptive estimation, fading channels, least mean square methods, prediction methods.

I. INTRODUCTION

IN IS-136 digital mobile TDMA systems, a relatively low symbol rate and long data slots (6.67 ms) cause severe fading. In such 1900-MHz systems, one or two fading dips can be expected within each data slot. Furthermore, large variations in fading rates and frequency selectivity are encountered, so well designed channel estimators are crucial for obtaining adequate performance. Estimates obtained from training sequences (synchronization words) cannot be used within the whole slot and interpolation of channel estimates between training sequences [15] here provides inadequate performance. The same is true for decision-directed LMS and RLS adaptation. A Kalman filter with time-varying gain [3] would provide optimal performance, but it requires an on-line update of the adaptation gain in every sample. This solution has so far been deemed too complex.

The Wiener LMS (WLMS) algorithm, which has constant gain but can efficiently utilize the fading statistics, was presented in Part I of this paper [14]. It enables a systematic and structured design of high-performance adaptation laws with LMS computational complexity. An early design related to this class of algorithms [10] has been successfully applied to tracking problems in IS-136 TDMA systems [1], [8], [19].

We will here investigate the application of WLMS algorithms to the estimation of such fading channels. With large variations in the fading rate, a key issue is the selection of appropriate statistical fading models (*hypermodels*). Several design approaches can be conceived, some of which are listed below in decreasing order of complexity.

1) An autoregressive model for fading channel taps may be adjusted on line. This estimator can be implemented jointly with a WLMS algorithm or a Kalman tracker [25].
2) Some fading models, in particular Jakes' model [7], are specified by a few parameters, such as the speed of the mobile, which may be estimated separately. A set of WLMS algorithms can be pre-designed within a grid of these and other parameters. The parameters are estimated on line and the appropriately tuned algorithm is selected. This *grid approach* [6] is sometimes called gain scheduling.
3) A single robustly designed algorithm might provide adequate performance over a wide range of Doppler shifts and disturbance levels.

At present, we consider alternative 1 to be far too complex and possibly nonrobust. The grid approach seems reasonable and has in [6] been found to work well. The use of a single fixed adaptive algorithm may at first sight seem over-optimistic, but it turns out to be feasible. The present paper will explore properties of the WLMS algorithm which are relevant when using either a grid approach or a single robustly designed tracker.

The channel model will be outlined in Section II and in Section III, the WLMS algorithm is summarized. Section IV describes the choice of hypermodel structure. It then discusses the adjustment of autoregressive models to the fading statistics generated by isotropic scattering, for known as well as for uncertain Doppler frequencies.

Analytical expressions for the steady state mean square parameter tracking error are presented in Section V. In this case study, with a two-tap fading channel and a symbol alphabet with constant modulus, an *exact* performance analysis can be performed.

In Section VI, the tracking performance is investigated for fading rates at which the adaptation laws are tuned, as well as for other fading rates. The use of predicted channel estimates is also investigated and is shown to improve the performance significantly.

The bit error rate performance is finally evaluated by simulation in Section VII, for adaptive Viterbi detectors working in decision-directed mode. A peculiar nonlinear effect that appears when estimating flat fading channels is here discovered and discussed.

II. THE CHANNEL MODEL

A sampled symbol-spaced baseband radio channel is described by the time-varying linear regression

$$y_t = (u_t \ldots u_{t-M+1}) \begin{pmatrix} h_{0,t} \\ \vdots \\ h_{M-1,t} \end{pmatrix} + v_t = \varphi_t^* h_t + v_t \quad (1)$$

where y_t, here assumed to be a scalar[1], is the received signal at discrete time t. The complex-valued fading M-tap channel is represented by h_t. In IS-136 systems, it is reasonable to assume $M = 1$ (flat fading) or $M = 2$. The symbols $\{u_t\}$ are assumed to have zero mean and constant modulus. The regressor vector φ_t^* is defined as the complex conjugate transpose of a column vector φ_t that appears in the adaptation algorithms. It is assumed stationary with a known nonsingular autocorrelation matrix $\mathbf{R} = E\varphi_t\varphi_t^*$. The noise v_t has zero mean and variance σ_v^2.

The fading properties of the channel coefficients will depend on the maximum Doppler frequency

$$\omega_D = 2\pi f_D = \frac{2\pi v_o}{\lambda} \quad \text{rad/s} \quad (2)$$

where v_o denotes the speed of the mobile and λ is the carrier wavelength, which in the following is assumed to be 16 cm ($\sim$1900 MHz). For the purpose of our channel estimator design demonstrations, we mainly assume Jakes' fading model [7]. When v_o is constant, the channel coefficients will then be stationary, circular Gaussian processes with zero means and covariance function

$$r_h(\ell) = Eh_t h_{t-\ell}^* = \mathbf{R}_h J_0(\Omega_D \ell) \quad \ell = 0, \pm 1, \ldots \quad (3)$$

which yields the classical fading spectrum

$$\phi_h(\Omega) = \begin{cases} \frac{2}{\sqrt{\Omega_D^2 - \Omega^2}}\mathbf{R}_h & |\Omega| < \Omega_D \\ 0 & |\Omega| > \Omega_D \end{cases}. \quad (4)$$

Here, $\mathbf{R}_h = Eh_t h_t^*$, while $J_0(\cdot)$ denotes the Bessel function of the first kind and zero order and

$$\Omega = \omega T \; ; \; \Omega_D = \omega_D T. \quad (5)$$

The symbol time T will be set to 41.15 μs as in IS-136.

III. THE CHANNEL ESTIMATOR

We shall use the WLMS-algorithm presented in Part I of this paper [14] to track and predict the channel h_t. To describe h_t, we shall use simplified fading models in the form of marginally

---

[1]The tracking and equalization algorithms are applicable also to vector signals, which appear in multiple antenna systems and when sampling faster than the symbol rate. See [12] for a design example.

stable autoregressive models of order n_D, with equal dynamics for all channel taps

$$\bar{h}_t = \frac{1}{D(q^{-1})}\mathbf{I}e_t = \frac{1}{1 + d_1 q^{-1} + \cdots + d_{n_D}q^{-n_D}}\mathbf{I}e_t. \quad (6)$$

The notation $\bar{h}_t$ is introduced to indicate that (6) will not be a perfect description of h_t. Here, q^{-1} denotes the backward shift operator ($q^{-1}y_t = y_{t-1}$) and e_t is a white zero mean random vector sequence with covariance matrix $\mathbf{R}_e$. For symmetric fading spectra, the scalar coefficients $\{d_i\}$ can be assumed real-valued.

The model (6) should approximate the essential behavior of the time variability, in our case described by the autocorrelation function (3). When (6), $\mathbf{R}_e$, $\mathbf{R}$ and σ_v are given, Theorem 1 of [14] directly provides an optimized WLMS-algorithm for tracking the parameter vector h_t in (1)

$$\varepsilon_t = y_t - \varphi_t^* \hat{h}_{t|t-1} \quad (7)$$

$$\hat{h}_t = \hat{h}_{t|t-1} + \mu \mathbf{R}^{-1}\varphi_t\varepsilon_t \quad (8)$$

$$\hat{h}_{t+k|t} = \frac{Q_k(q^{-1})}{Q_0(q^{-1})}\mathbf{I}\hat{h}_t. \quad (9)$$

Here, $\hat{h}_{t+k|t}$ denotes an estimate of h_{t+k} at discrete time t and $\hat{h}_t = \hat{h}_{t|t}$. The scalar gain μ is a step size parameter and (9) is the coefficient smoothing-prediction estimator. An alternative equivalent implementation can be expressed in terms of the *learning filter* $\mathcal{L}_k(q^{-1})$ [14]:

$$f_t = \mathbf{R}\hat{h}_{t|t-1} + \varphi_t\varepsilon_t$$

$$\hat{h}_{t+k|t} = \mathcal{L}_k(q^{-1})f_t = \frac{Q_k(q^{-1})}{\beta(q^{-1})}\mathbf{R}^{-1}f_t. \quad (10)$$

where

$$\beta(q^{-1}) = D(q^{-1}) + q^{-1}Q_1(q^{-1}).$$

The polynomials $Q_i(q^{-1})$ depend on the selected hypermodel (6) and are calculated via Theorem 1 in [14] to minimize the mean square parameter error

$$E|\tilde{h}_{t+k|t}|^2 = tr(E\tilde{h}_{t+k|t}\tilde{h}_{t+k|t}^*) \triangleq tr(\mathbf{P}_k) \quad (11)$$

where

$$\tilde{h}_{t+k|t} = h_{t+k} - \hat{h}_{t+k|t}.$$

IV. DYNAMIC FADING MODELS

A. Autoregressive/Integrating Models

An exact representation of the fading statistics (3)–(4) would require the use of an autoregressive fading model (6) of infinite order. We will here use and compare the following special cases of (6).

1) **RW**, Random walk modeling, $D(q^{-1}) = 1 - q^{-1}$, results in an LMS algorithm. It is a common first choice when no prior information is available[2].

---

[2]However, in such cases we would rather advocate the use of filtered random walk modeling, see below, with $a \in [0.9$–$0.999]$.

2) **FRW** (Filtered random walk):

$$D(q^{-1}) = (1 - q^{-1})(1 - aq^{-1}),$$

with $|a| \leq 1$, is a useful model in many situations. The special case of an integrated random walk (**IRW**, $a = 1$), will be appropriate if the short term behavior is well approximated by linear trends.

3) **AR$_2$** (Autoregressive second order model):

$$D(q^{-1}) = 1 - 2\rho \cos \omega_o q^{-1} + \rho^2 q^{-2}.$$

Here, ρ and ω_o determine the degree of damping and the dominating frequency, respectively. For Jakes fading models (3), a reasonable bandwidth is obtained with $\omega_o = \Omega_D^o/\sqrt{2}$ where Ω_D^o is a nominal or estimated Doppler frequency.

4) **AR$_2$I** (Autoregressive and integrating model):

$$D(q^{-1}) = \left(1 - 2\rho \cos \frac{\Omega_D^o}{\sqrt{2}} q^{-1} + \rho^2 q^{-2}\right)(1 - q^{-1}).$$

This model is useful when some parameters are oscillating while others are slowly varying or constant. The integrating term $(1 - q^{-1})$ will guarantee an unbiased estimate of constant parameters when $\mathbf{R}$ is nonsingular, see [14, eq (42)]. The AR_2I model is also of use for long-range prediction of oscillations around a nonzero mean, which occurs in Rician fading; without an integrating model factor, prediction estimates would in that case be biased toward zero.

5) **AR$_{n_D}$**, autoregressive models of order $n_D = 3$ or higher, are appropriate when important properties of the covariance function of the time-variation are difficult to match with a few parameters. Their adjustment is described in Section IV-B.

Design based on RW modeling results in an LMS algorithm, while FRW or AR_2 modeling leads to a simplified Wiener LMS algorithm, which is simple to design and to readjust on-line, see Section IV of [14]. With AR_2I or AR_{n_D} models, readjustment of the algorithm (at most once per slot) will require the numerical solution of a polynomial spectral factorization of order n_D.

When using AR_2 and AR_2I models, we need to select the parameters Ω_D^o and ρ. In this case study, the pole radius ρ is fairly easy to select. For maximum normalized Doppler frequencies of interest here, $\Omega_D < 0.1$, the value $\rho = 0.999 - 0.1\Omega_D$ is by our experience reasonable for Jakes' model. Then, Ω_D^o is set to Ω_D which can be estimated on line reasonably well using either the assumed correlation Bessel function (3) of the fading pattern [11], or level crossing rates.

B. Adjusting AR Model Parameters to Fading Covariance Statistics

The adjustment of (6)

$$\bar{h}_t + d_1 \bar{h}_{t-1} + \cdots + d_{n_D} \bar{h}_{t-n_D} = e_t \tag{12}$$

can be based directly on a known or estimated covariance function. We can adjust $D(q^{-1})$ by considering row j of (12). Introduce the set of covariances

$$\{\bar{r}_{\ell_i} \triangleq E\bar{h}_{j,t} \bar{h}_{j,t-\ell_i}^*\}_{i=1}^N,$$

where $\bar{h}_{j,t}$ denotes element (tap) j of $\bar{h}_t$ and where ℓ_i are integers such that $0 < \ell_1 < \cdots < \ell_N$. Multiplying row j of (12) by $\bar{h}_{j,t-\ell_i}^*$ and taking the expectation gives the equations

$$\bar{r}_{\ell_i} + d_1 \bar{r}_{\ell_i - 1} + \cdots + d_{n_D} \bar{r}_{\ell_i - n_D} = 0 \quad i = 1, 2, \ldots, N. \tag{13}$$

In the particular case of $\ell_i = i$ and $N = n_D$, we obtain the Yule-Walker equations. However, N might very well be chosen much larger than n_D and the time-lags ℓ_i can be distributed over a large interval.

The covariances $\bar{r}_j$ can be replaced by data-based estimates. The resulting polynomial $D(z^{-1})$ could then have roots outside the unit circle and should in that case be adjusted so that all roots are in $|z| \leq 1$. Estimation of $\bar{r}_j$ based on data, as suggested in [25], will require an initial training period of considerable length and will give reliable estimates only at high SNR's.

We therefore prefer to use theoretical expressions for the covariances, parametrized by the maximum Doppler frequency. When adjusting the AR model to the fading model (3), we replace $\bar{r}_{\ell_i - w}$ in (13) by $J_0(\Omega_D(\ell_i - w))$ and solve the possibly over-determined system of equations by the least squares method.

In Fig. 1, the Bessel function in (3) for $\Omega_D = 0.02$ (45 km/h) is compared to the AR_3 covariance function adjusted with $N = 6$, for $\ell_N = 61$ and $\ell_N = 251$. Clearly, including higher-lag covariances in (13) yields a better agreement between the Bessel function and the AR model for large lags.

The correlation between taps, modeled by $\mathbf{R}_h$ in (3) and $\mathbf{R}_e$ in (6), can be estimated from data. With well synchronized IS-136 receivers, the tap correlation will be small.

C. Robust Design of Adaptation Laws

If the Doppler frequency Ω_D is uncertain, one could minimize the worst-case effect of this uncertainty by performing a minimax robust filter design [9], [18]. A less conservative and often much less computationally demanding, alternative is to regard Ω_D as a random variable. The MSE tracking performance resulting from the outcomes of Ω_D is averaged and we minimize this average [23], [26]. As is shown in [24] and [11, Sect. 3.5], this problem can be solved by spectrally *averaging over the hypermodels* (6). Such averaging has also been used in [17, Sect. IV.A]. A Doppler spectrum averaged with respect to an uncertain parameter Ω_D is given by

$$\tilde{\phi}_h(\Omega) \triangleq E\phi_h(\Omega) = \int_{-\pi}^{\pi} \phi_h(\Omega, \Omega_D) p(\Omega_D) \, d\Omega_D \tag{14}$$

where $\phi_h(\Omega, \Omega_D)$ represents the spectrum of the channel coefficients and $p(\Omega_D)$ denotes the probability density function of the normalized maximum Doppler frequency Ω_D. When assuming
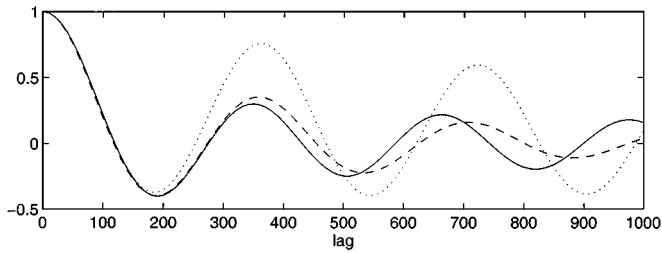
Fig. 1. Adjusting third-order AR hypermodels to the Bessel function $J_0(\Omega_D\ell)$, at $\Omega_D = 0.02$ (45 km/h), (solid) according to (13) at six evenly spaced points, for the maximum lag $\ell_N = 61$ (dotted) and $\ell_N = 251$ (dashed).

Fig. 2. Autocovariance function $r_h(\ell) = J_0(\Omega_D\ell)$ with $\Omega_D = 0.02$ (solid) and the averaged covariance function (15), with $\Omega_D \in U[0.01\ 0.03]$ (dotted) and $\Omega_D \in U[0.015\ 0.025]$ (dashed).

Jakes model and (3), the covariance function corresponding to (14) is

$$\tilde{r}_h(\ell) \triangleq \int_{-\pi}^{\pi} r_h(\ell)p(\Omega_D)d\Omega_D$$

$$= \int_{-\pi}^{\pi} \mathbf{R}_h J_0(\Omega_D\ell)p(\Omega_D)d\Omega_D \qquad (15)$$

An averaged AR hypermodel can now be adjusted using $\tilde{r}_h(\ell)$ instead of $\bar{r}_h(\ell)$. A robust tracking algorithm can then be designed using this model.

In Fig. 2, the averaged covariance function (15) is displayed for a uniformly distributed probability density function $p(\Omega_D)$ with different uncertainty regions. A wider uncertainty region will increase the damping of the averaged covariance function, yielding a spectrum with a less pronounced peak.

Deviations from Jakes' model can be regarded as unstructured uncertainty, which can be incorporated in an averaged robust design, see [11], [23], [26].

V. PERFORMANCE ANALYSIS

Based on *two-tap* channel models (1) and on a known fading model such as Jakes' model (3), we can obtain an exact expression for the steady state tracking MSE, $tr\mathbf{P}_k$. The expression is valid for arbitrarily fast fading and for all algorithms with WLMS structure. Introduce the learning filter gain

$$\Sigma_k = \frac{1}{2\pi} \int_{-\pi}^{\pi} \left| \frac{Q_k(e^{j\Omega})}{\beta(e^{j\Omega})} \right|^2 d\Omega. \qquad (16)$$

Lemma 1: Consider the channel model (1), with $M < 3$. Assume h_t, φ_t^* and v_t to be mutually independent and stationary. Let the fading channel coefficient vector have spectrum $\phi_h(\Omega)$ and covariance matrix $Eh_t h_t^* = \mathbf{R}_h$. The zero mean noise v_t has variance σ_v^2. Let the zero mean symbols u_t be uncorrelated in time, with constant modulus and variance σ_u^2 ($\mathbf{R} = \sigma_u^2\mathbf{I}$). Assume $(M-1)\Sigma_1 < 1$. If an estimator for h_{t+k} with the structure (10) or (7)–(9) is used, then the steady-state mean square estimation error (11) is given by

$$tr\mathbf{P}_k = \frac{\Gamma_k + M10^{-\frac{SNR}{10}}\Sigma_k + (M-1)G_k}{1 - (M-1)\Sigma_1}tr\mathbf{R}_h \qquad (17)$$

where

$$\Gamma_k = \frac{1}{2\pi} \int_{-\pi}^{\pi} \left| \frac{\beta(e^{j\Omega}) - e^{j\Omega k}Q_k(e^{j\Omega})}{\beta(e^{j\Omega})} \right|^2 \frac{tr\phi_h}{tr\mathbf{R}_h}d\Omega \quad (18)$$

$$G_k = \Gamma_1\Sigma_k - \Gamma_k\Sigma_1 \qquad (19)$$

and

$$SNR \triangleq 10\log\frac{\sigma_u^2}{\sigma_v^2}E|h_t|^2 \qquad \text{(dB)} \qquad (20)$$

$\square$

Proof: Obtained from [13] for constant modulus regressors (with kurtosis 1), by observing that $tr\mathbf{V}_h^k = tr(\mathbf{R}_h)\Gamma_k$ and $E|h_t|^2 = tr\mathbf{R}_h$.

Lemma 1 holds exactly for $M < 3$, but is a good approximation also for higher order FIR channels.

Above, $(M-1)\Sigma_1 < 1$ is a condition for convergence in MSE. This condition will always be fulfilled for flat fading channels. Note also that the term G_k vanishes for $k = 1$. All preconditions for Lemma 1 are fulfilled in the IS-136 TDMA system: The symbols u_t are uncorrelated due to the interleaving and are circular with constant modulus. The delay spread is not larger than one symbol interval T, so channel models with $M \leq 2$ are appropriate. The term v_t represents mainly co-channel interference and thermal noise. It can be assumed zero mean and independent of both u_τ and h_τ for all τ.

For filters and smoothers (7)–(9) designed to minimize (11) based on perfect models, the error will vanish with a vanishing noise variance.

For predictors, the tracking error (17) will not vanish even in the noise-free case and it will increase with the fading rate. It decreases if more accurate AR-approximations of the true fading spectrum ϕ_h are used in the WLMS design.

It is of interest to know to what extent improved linear regression modeling of the parameter dynamics can improve the end result for which it is intended. Filtering or detection performance is essentially determined by the ambient SNR. With Lemma 1, the variance of the "tracking noise" $\sum_{i=0}^{M-1} \tilde{h}_{i,t|t-k}u_{t-i}$, caused by nonperfect tracking, can be calculated and compared to the variance of the noise v_t. As a rough but useful performance indicator, we define the relative noise level

$$V \triangleq 10\log\left(\frac{\sigma_u^2 tr\mathbf{P}_k + \sigma_v^2}{\sigma_v^2}\right) \qquad \text{(dB)} \qquad (21)$$

where the numerator describes the variance in $y_t - \varphi_t^*\hat{h}_{t|t-k}$ due to the tracking error plus noise, if $\tilde{h}, u$ and v are mutually uncorrelated. We can use the increase of the noise level to predict the performance deterioration in e.g., an equalizer[3].

[3]A similar investigation is performed for Kalman trackers and decision feedback equalizers in [22].
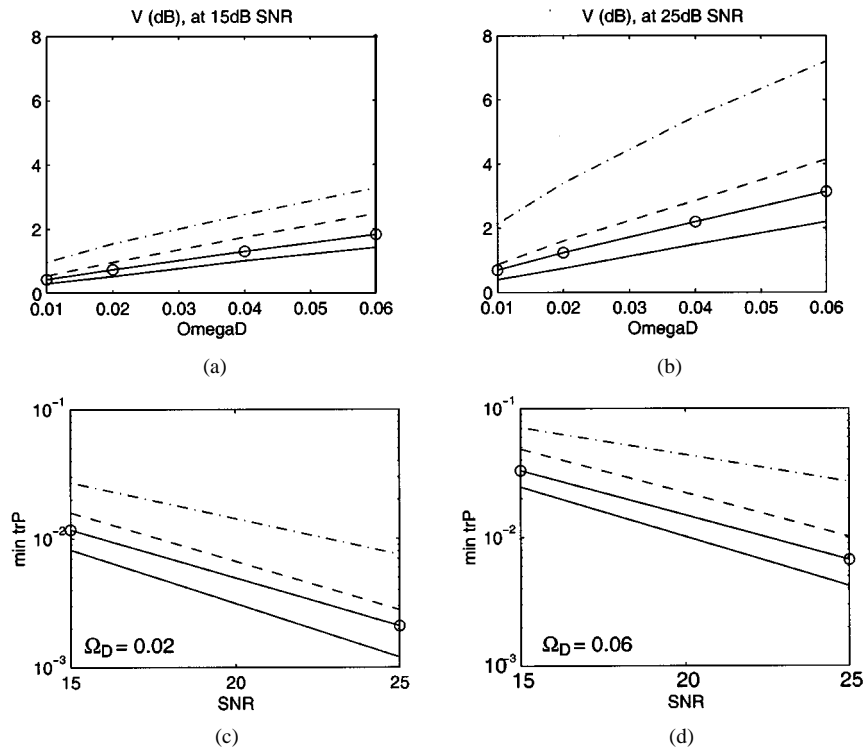
Fig. 3. Optimized tracking error $E\|\bar{h}_{t+1|t}\|_2^2 = tr\,\mathbf{P}_1$ (lower part) and relative tracking noise level V (dB) (upper part) in Section VI for WLMS algorithms based on RW modeling (dashed-dotted), IRW (dashed) AR_2 (circles) and AR_4 (solid). All AR models are matched to the true normalized Doppler frequency Ω_D.

TABLE I
THE ATTAINABLE TRACKING ERROR $tr\,\mathbf{P}_1$ OBTAINED BY LEMMA 1 FOR WLMS ALGORITHMS BASED ON DIFFERENT HYPERMODELS MATCHED TO THE TRUE DOPPLER FREQUENCY. FOR FRW, $a = 0.98$. COMPARE TO FIG. 3

Ω_D	0.01		0.02		0.04		0.06	
SNR	15 dB	25 dB	15 dB	25 dB	15 dB	25 dB	15 dB	25 dB
RW	0.0159	0.0040	0.0271	0.0075	0.0485	0.0160	0.0711	0.0269
FRW	0.0101	0.0019	0.0161	0.0030	0.0292	0.0058	0.0447	0.0096
IRW	0.0086	0.0014	0.0159	0.0028	0.0312	0.0059	0.0484	0.0101
AR_2	0.0067	0.0011	0.0117	0.0021	0.0218	0.0042	0.0329	0.0067
AR_2I	0.0057	0.0009	0.0108	0.0016	0.0203	0.0034	0.0329	0.0055
AR_3	0.0050	0.0008	0.0092	0.0014	0.0175	0.0030	0.0264	0.0048
AR_4	0.0047	0.0006	0.0082	0.0012	0.0165	0.0026	0.0245	0.0042

When V is above 3 dB, the tracking noise dominates over the output noise v_t. It is then worthwhile to consider a superior adaptation law based on, for example, a higher order hypermodel. If V is below 1 dB, then the noise v_t dominates, so even a total elimination of the tracking errors would result in marginal improvements of the performance of a filter or detector based on the estimated model.

VI. MSE PERFORMANCE

We will here investigate the performance of the tracking algorithm theoretically, by using Lemma 1 for two-tap Rayleigh fading channels with taps of equal variance and regressors with constant modulus and variance 1.

A. MSE Performance: The Ideal Case

In the lower half of Fig. 3, the mean square sum of tap prediction errors $tr\,\mathbf{P}_1$ has been calculated by Lemma 1, using ϕ_h from (4) and $tr\,\mathbf{R}_h = 2$. We investigate WLMS algorithms based on adjusted hypermodels of various structures, with optimized gains μ, for SNR of 15–25 dB. The corresponding numerical results are presented in Table I. While the attainable performance improves with the complexity of the hypermodel, the use of increasingly complex models gives diminishing returns.

The top diagrams in Fig. 3 display the relative tracking noise level (21), under the assumption $\sigma_u^2 = 1, E|h_t^o|^2 = E|h_t^1|^2 = 1$ and $SNR = 10\log(2/\sigma_v^2)$. For LMS tracking (WLMS based on random walks), the tracking error is in many of the considered

(a)

(b)

(c)

(d)
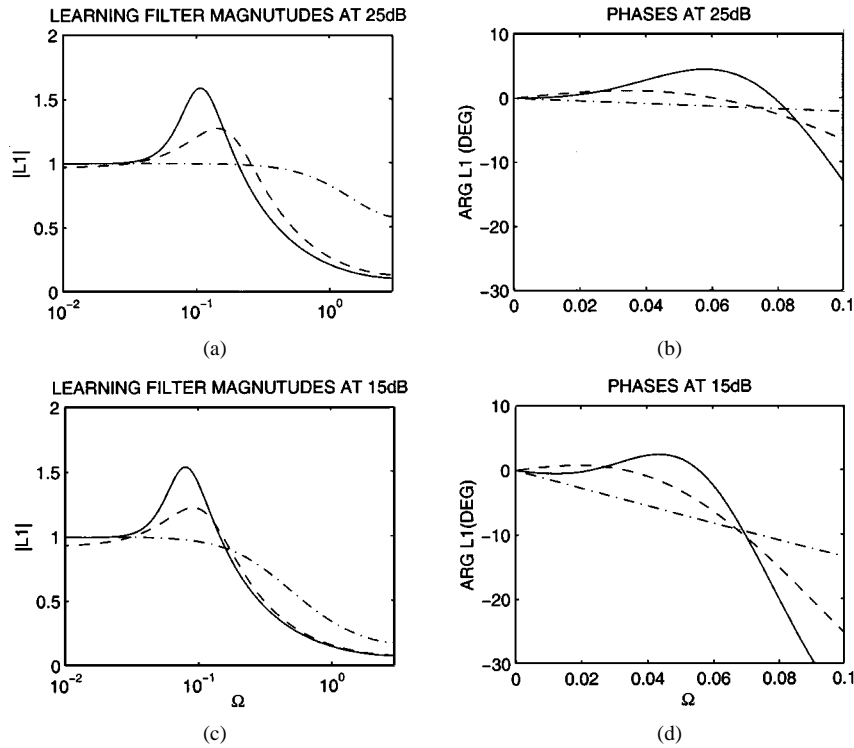
Fig. 4.   Learning filter magnitudes $|Q_1(e^{i\Omega})/\beta(e^{i\Omega})|$ (left) and phases (right) for optimally tuned WLMS algorithms based on RW (dash-dotted) AR_2 (dashed) and AR_2I (solid) fading models at $\Omega_D = 0.04$ ($f_D = 160$ Hz), for $SNR = 25$ dB and $SNR = 15$ dB, respectively.

cases so large that it dominates over v_t ($V > 3$ dB in the upper diagrams of Fig. 3). The tracking performance can be improved significantly by simply extending LMS (RW hypermodeling) with an integrator, i.e., by using an IRW hypermodel. If we use an AR_4 model, we obtain a better tracking MSE for $\Omega_D = 0.06$ (~ 140 km/h) than can be obtained by using the RW model with $\Omega_D = 0.02$ (~ 45 km/h). In terms of the effect of the noise level on the tracking MSE, more than 10 dB can be gained at both $\Omega_D = 0.02$ and $\Omega_D = 0.06$ by using an AR_4 model instead of a random walk model (bottom diagrams).

The properties of different adaptation algorithms can also be understood by comparing their learning filters (10). See Fig. 4, which compares RW (LMS), AR_2 and AR_2I designs at $\Omega_D = 0.04$.[4] The bandwidth of the learning filter approaches $\Omega_D = 0.04$ as the SNR decreases but, as can be seen in Fig. 4, it is significantly higher for moderate and high SNR's. The reason is that the lag error will, to a large extent, be determined by the phase lag introduced by the learning filter in frequency regions where h_t has significant energy. When the noise level is low, a Wiener design can give priority to suppressing lag errors by attaining low phase shifts at these frequencies (at or below $\Omega_D = 0.04$), at the price of widening the bandwidth of the learning filter. When the SNR decreases, noise rejection is given higher priority.

Note that the RW/LMS learning filter has the highest gain at high frequencies. This makes this estimator most sensitive to noise.

B. Mismatched Designs

The performance of incorrectly tuned algorithms has also been computed from Lemma 1 and are presented in Table II. From Table I and Table II, we can draw the following conclusions.

- If the Doppler frequency Ω_D is uncertain, AR_2I modeling seems to be the best choice when Ω_D is overestimated. When Ω_D is underestimated, AR_3 models appear to perform slightly better. (Bold numbers in Table II.)
- The use of a higher order AR hypermodel results in considerably better tracking performance than the use of a RW model, even if Ω_D^o is severely mismatched in the latter case (Table I, Table II).

In Fig. 5, the tracking algorithms were matched to a maximum Doppler frequency of 140 Hz ($\Omega_D = 0.035$) and an SNR of 15 dB. These results indicate that the AR_2I hypermodel is a superior choice if we *underestimate* the SNR and *overestimate* the Doppler frequency.

The bottom line of the evaluation so far can be formulated as follows: *If an uncertain estimate of Ω_D is available and low computational complexity is required, then use a WLMS algorithm based on a nominal AR_2I hypermodel.* Select the design value Ω_D^0 at the high end of the uncertainty interval of Ω_D and the design value of the SNR at the lower limit of its uncertainty range. Such a design should provide good performance for all Doppler frequencies from zero up to Ω_D^0.

The robust averaged design proposed in Section IV-C has been investigated on IS-136 channels in [24], based on averaged AR_3 hypermodels. It turned out to give a further reduction of the averaged tracking MSE, as compared to designing for the maximal Ω_D^0.

[4]The tuned second order AR denominator is given by $D(q^{-1}) = 1 - 1.9891q^{-1} + 0.99003q^{-2}$. For 25 dB, the tuned step length parameters μ are 0.36, 0.21 and 0.17 for RW, AR_2 and AR_2I-based designs, respectively. For 15 dB, $\mu = 0.27$, 0.13 and 0.127, respectively.

TABLE II
AS IN TABLE I BUT FOR HYPERMODELS MATCHED TO THE FADING STATISTICS FOR AN INCORRECT DOPPLER FREQUENCY. THE MINIMAL VALUES OF EACH COLUMN ARE EMPHASIZED

	AR_{n_D} matched to $\Omega_D = 0.02$				AR_{n_D} matched to $\Omega_D = 0.04$			
Ω_D	0.01		0.04		0.01		0.02	
SNR	15 dB	25 dB	15 dB	25 dB	15 dB	25 dB	15 dB	25 dB
AR_2	0.0122	0.0021	0.0279	0.0053	0.0257	0.0049	0.0231	0.0044
AR_2I	**0.0085**	**0.0013**	0.0287	0.0045	**0.0129**	**0.0022**	**0.0154**	**0.0025**
AR_3	0.0100	0.0015	**0.0260**	**0.0042**	0.0193	0.0033	0.0199	0.0034
AR_4	**0.0085**	**0.0013**	0.0285	**0.0042**	0.0185	0.0029	0.0182	0.0029
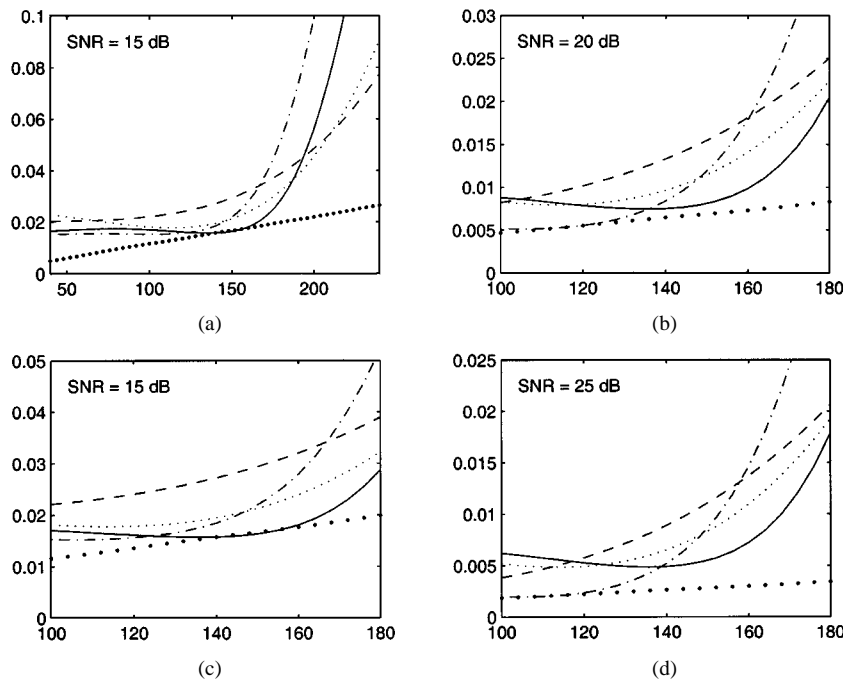
Fig. 5. MSE performance $tr\,\mathbf{P}_1$ as a function of f_D for different choices of WLMS algorithms *matched to 140 Hz and 15 dB*. The algorithms are based on IRW (dashed), AR_2 (dotted), AR_2I (dash-dotted) and AR_3 (solid) hypermodels. Compare to a fully matched AR_3 design (bulleted). The lower left-hand plot expands the upper left-hand diagram.

C. Optimal Channel Prediction

Optimized channel predictors can be designed using either Kalman trackers or WLMS algorithms[5]. Fig. 6 illustrates the MSE performance obtained by using AR_3 prediction (circles) instead of just extrapolating the current estimate into the future (crosses). The improvement is large and it increases with the prediction length. Naturally, the gain will increase with an increasing vehicle speed and a decreasing noise level. Similar, but somewhat smaller improvements were obtained when using AR_2I and AR_2 hypermodels.

The use of this type of linear prediction can also be of interest e.g., for fast power control in CDMA systems. Long-range prediction is of interest for resource scheduling and adaptive modulation [4], [5].

[5]The use of e.g an LMS filter estimate and a separate predictor for this time series [2] is a suboptimal alternative.

VII. SIMULATION STUDY

We shall investigate the bit error rate performance of adaptive decision-directed Viterbi receivers, as described by Fig. 7. The channel estimator utilizes estimated symbols as regressors in decision-directed mode. It provides predicted channel taps, which are used in the metric computation of the Viterbi algorithm.

For adaptive detectors working in decision directed mode, the tracking is required to be accurate and robust against erroneous regressors, which will occur in particular around fading dips, where $|h_t|$ is small.

A. Specifications

We focus on a setup suitable for the IS-6 standard [20], with the following conditions.
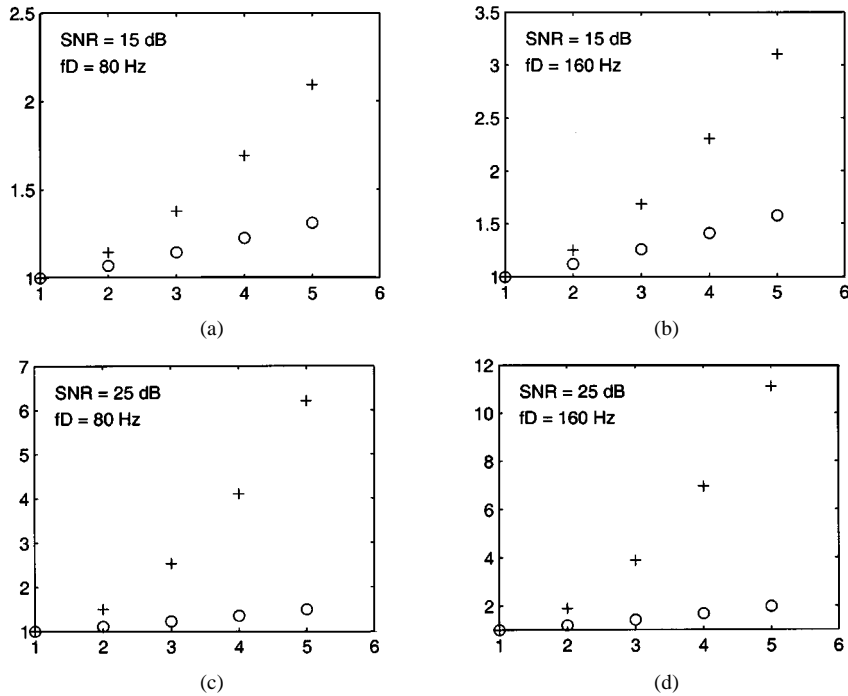
Fig. 6. Relative MSE increase $\mathrm{tr}\mathbf{P}_k/\mathrm{tr}\mathbf{P}_1$, of k-step channel prediction of Rayleigh fading channel taps, compared to one-step prediction, as a function of k. The most recent channel estimate used as k-step predictor (crosses) is compared to the use of an optimal k-step predictor (circles), for AR_3-based WLMS tracking algorithms.
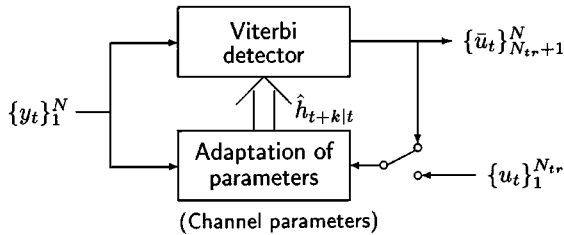
Fig. 7. Adaptive equalization based on decision directed channel estimation. In learning-directed mode, the adaptation is based on training data. At time instant $t = N_{tr} + 1$, the adaptation is switched into decision-directed mode and decisioned symbols $\bar{u}_t$ are used as regressor variables.

- *Slot structure:* As in the forward link of IS-136 with $N = 162$ differential QPSK-modulated symbols, including $N_{tr} = 14$ leading training symbols.[6]
- *Channel properties:* A two tap Rayleigh fading symbol-spaced baseband channel model with independently fading taps[7] is simulated

$$y_t = h_{0,t}u_t + h_{1,t}u_{t-1} + v_t \; ; \; \mathbf{R} = \mathbf{I} \qquad (22)$$

with $\mathbf{R}_e$ diagonal and $E|h_{0,t}|^2 = E|h_{1,t}|^2 = 1$. The taps $h_{i,t}$ are generated according to [7], using 12 offset oscillators with uniformly distributed ($[0, 2\pi]$) phases. Hence, the level crossing statistics is close to that of a classical Rayleigh fading environment. All estimators are initialized from least squares estimates of the channel taps in

the form of robustified linear trends, based on the initial training sequence[8]. We also study the flat fading case.

- *Disturbance properties:* The scenario is interference-limited with burst-synchronized interferers propagating via the same type of fading channel as the signal. In the simulations, the interference was also symbol-synchronized. The color of the interference is not estimated. (In a noise-limited scenario with Gaussian noise, the BER performance improves.)
- *Idealized simulation conditions:* To isolate the tracking properties, we have compared decision directed adaptation to the use of correct symbols u_t as regressors. To quantify the loss of performance due to imperfect initialization, we also compare to initialization with known channel taps.

B. BER Performance at 90 km/h

WLMS tracking algorithms based on random walk (LMS), AR_2 and AR_2I fading models are now evaluated in combination with a Viterbi algorithm at $\Omega_D = 0.04$, or $f_D = 160$ Hz (speed 90 km/h).

We use a recursively updated Viterbi detector [8], [11], [21] which needs to process its input over a few samples before a reliable symbol decision can be reached. A decision delay of three steps here provides the best performance. Due to an additional

---

[6]A known CDVCC sequence of six differential symbols is placed after 85 symbols of the slot. It is here not used to improve the tracking performance, since this would complicate the performance evaluation.

[7]The more realistic case of correlated taps would result in higher bit error rates due to partial loss of diversity, but will otherwise not provide any new fundamental problems for the tracking.

[8]Since the slope of a linear trend will be more uncertain than its average level, we initialize the model as

$$\hat{y}_t = (h_{0,\ell} + (t-8)\alpha h_{0,s})u(t) + (h_{1,\ell} + (t-8)\alpha h_{1,s})u(t-1);$$
$$t = 2 \dots 15$$

where $\alpha = SIR/22$ for $0 < SIR < 22$ dB, with SIR being the signal-to-interference ratio estimated from the model residuals during the training phase. Here, $h_{i,\ell}$ and $h_{i,s}$ are estimated jointly by off-line least squares. The robustification parameter α de-emphasizes uncertain slope estimates at low SIR's.
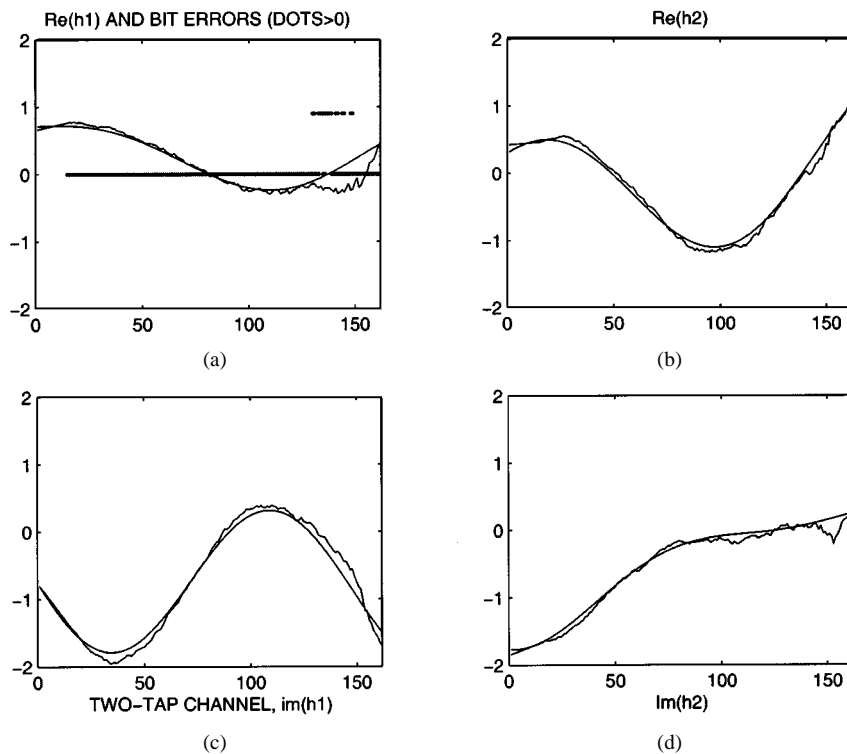
Fig. 8. Real and imaginary parts of tap 1 and tap 2, showing true trajectories and estimates by an AR_2I-designed WLMS algorithm at $SIR = 20$ dB. In the upper left figure, dots at the zero level symbolize correct decisions while dots at level 0.9 indicate decision errors.

unavoidable delay in the regressor feedback loop, channel prediction $k = 4$ steps ahead is then required. For LMS, a decision delay of two steps provided the best performance.

Fig. 8 illustrates a rather typical tracking and bit error performance obtained at 20 dB with AR_2I-based tracking. The estimates are initialized as linear trends. Everything goes well until the fading dip occurs at sample ~ 130, leading to several decision errors. When these errors are fed back as regressors to the tracker, they disturb the tracking in the interval 130–150. The system recovers after symbol no. 150.

More conclusions can be drawn from statistics on the BER when the correct Ω_D and signal-to-interference ratios (SIR's) are used in the design. Table III, supported by Fig. 9, presents the uncoded bit error rate for two-tap channels. Table IV illustrates the flat fading case.

The performance indicator V from (21) in Table III and Table IV provides adequate predictions of how much the BER plot for cases based on known regressors is shifted to the right, relative to the curve for a known channel.

Comparing the dotted to the lower dash-dotted curve in Fig. 9 we see that not much performance is lost due to imperfect initialization. (If the algorithms were initialized with levels instead of linear trends, the performance would deteriorate further by 1–2 dB.)

Decision-directed adaptation results in a performance loss due to nonlinear feedback effects caused by decision errors in the regressors. It is approximately 3dB for WLMS based on AR_2 and AR_2I models in Fig. 9.

In Table III and Fig. 9, WLMS based on AR_2I models show the best performance, but the performance of AR_2-based trackers is rather close. LMS tracking will in this case be
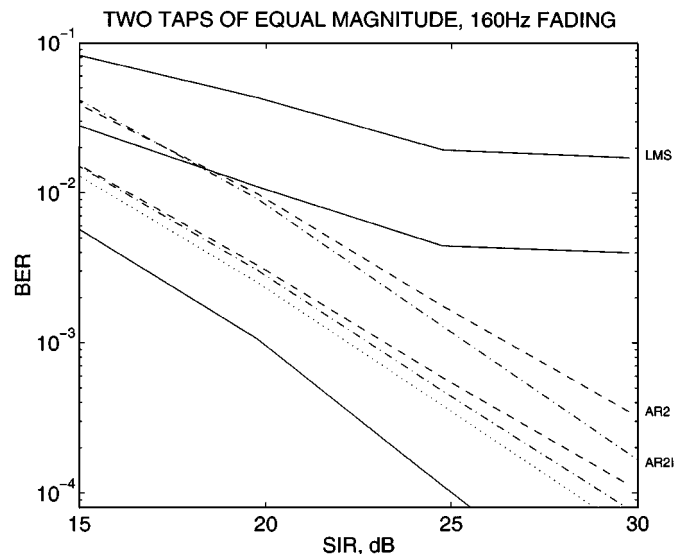
Fig. 9. The Bit error rate as a function of the signal-to-interference ratio for the adaptive Viterbi equalizer. The BER with correct channel (lower solid) is compared to WLMS tracking with AR_2I modeling with true u_t as regressors (lower dash-dotted) and estimated regressors (upper dash-dotted) and to WLMS tracking with AR_2 modeling with true u_t as regressors (lower dashed) and estimated regressors (upper dashed). Compare to LMS with optimized step length and true u_t as regressors (middle solid) and with estimated regressors (upper solid). Also shown is AR_2I tracking using true u_t and correct initialization (dotted).

completely inadequate, partly due to its inappropriate structure and not least due to its inability to predict the channels; With a random walk model, $\hat{h}_{t+k|t} = \hat{h}_{t|t}$. This results in a significant lag error, which will not vanish at low disturbance levels. Hence, the error floor at 1.7% BER. (Error floors also exist for

TABLE III

ADAPTIVE EQUALIZATION OF THE CHANNEL (22) AT $\Omega_D = 0.04$ WITH $E |h_{0,t}|^2 = E |h_{1,t}|^2 = 1$. 10 000 SLOTS PER SIMULATION CASE. IN THE LOWER PART OF THE SYMBOLS ARE USED IN φ_t^* IN THE CHANNEL ESTIMATORS. THE RIGHT-HAND COLUMNS SHOW OPTIMAL ADAPTATION GAINS μ AND RELATIVE TRACKING NOISE LEVELS (21) WITH PREDICTION HORIZON $k = 4$ ($k = 3$ FOR LMS)

	BER (%)			μ and V		
SIR (dB):	15	20	25	15	20	25
DECISIONED REGRESSORS:				μ:		
LMS	8.3	4.1	1.9	.31	.31	.36
WLMS AR2	4.0	.92	.17	.14	.18	.21
WLMS AR2I	4.0	.85	.12	.13	.15	.17
TRUE REGRESSORS:				V (dB):		
LMS	2.8	1.1	.62	5.8	9.0	13.1
WLMS AR2	1.5	.30	.054	3.1	4.3	5.8
WLMS AR2I	1.5	.28	.044	2.9	3.7	4.8
Known channel	0.58	.09	.010	0	0	0

TABLE IV

FLAT FADING AT $\Omega_D = 0.04$, $E |h_{0,t}|^2 = 1$, $E |h_{1,t}|^2 = 0$. 10 000 SLOTS ARE CONSIDERED FOR EACH SIMULATION CASE. IN ROW 4 TO 6, A TRUE SYMBOL IS USED AS REGRESSOR. THE RELATIVE NOISE LEVEL (V) IS OBTAINED WITH $k = 1$

	BER (%)			μ and V	
SNR (dB):	15	20	25	15	25
DECISIONED REGRESSORS:				μ:	
LMS	2.8	1.00	.36	.39	.73
WLMS AR2	2.7	0.95	.32	.17	.25
WLMS AR2I	2.7	0.96	.33	.14	.19
TRUE REGRESSORS:				V (dB):	
LMS	3.1	1.24	.52	1.5	3.2
WLMS AR2	3.2	1.12	.37	0.7	1.2
WLMS AR2I	2.5	0.88	.31	0.6	1.0
Known channel	2.1	0.69	.23	0	0

the AR_2 and AR_2I-based designs, but they are far below the BER levels investigated in Fig. 9.)

To test our conclusions from Section VI-B, we have designed AR_2 and AR_2I-based WLMS algorithms for $f_D = 160$ Hz and $SIR = 15$ dB and evaluated their performance at other operating points. The results, presented in Fig. 10, confirm that one single fixed adaptive filter, designed at the high end of the uncertainty interval of the Doppler frequency and the low end of the SIR range can indeed be used over the whole parameter range. If the operating area is considered to be bounded by $SIR = [15,25]$ dB and $f_D = [0, 160]$ Hz, this filter does in fact constitute a minimax robust design, since the so-called saddle-point condition [9] is fulfilled: The resulting performance attains its worst value at the nominal (worst-case) design point. In the most critical regions, with low SIR and/or high Doppler frequency, the performance for an AR_2I-based design is about the same as for an AR_2-based design.

In the flat fading case, with $h_{1,t} = 0$, not much can be gained by improving the tracking. An exception is at high SNR, where
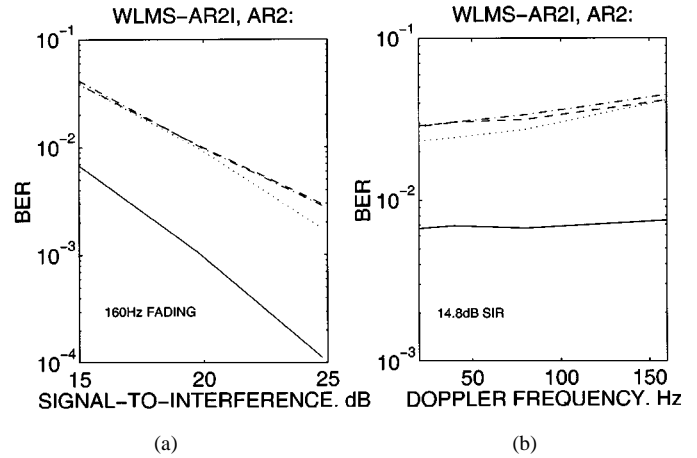
Fig. 10. The BER as function of the SIR at 160 Hz (left figure) and as a function of the Doppler frequency at 14.8 dB SIR (right figure) for an adaptive Viterbi detector with k=4 step prediction. Performance of AR_2I-based (dash-dotted) and AR_2-based (dashed) WLMS channel estimators, *designed for SIR = 15 dB and f_D = 160 Hz.* Compare to the performance of AR_2-based WLMS designed for the true SIR and f_D (dotted) and to the performance for a known channel (solid).

for true regressors a significantly lower BER is attained for AR_2 or AR_2I-based designs than for LMS. This can be predicted by the values of V from (21) in the right-hand part of Table IV. For flat fading channels, all the algorithms provide about the same performance. The detector becomes trivially simple, so no channel prediction beyond $k = 1$ is required.

One can note an oddity in the results in Table IV: The BER is in several cases *lower* when a decisioned symbol is used as regressor, $\hat{y}_t = \hat{h}_t \bar{u}_t$, as compared to using the correct symbol $\hat{y}_t = \hat{h}_t u_t$. This effect is peculiar to *flat fading* channels on which *differential detection* and adaptive decision-directed receivers with *high gain* are used. As verified by simulation, a single error in a differential symbol normally results in two consecutive bit errors with correct channel estimates. In this case, the large estimation error ε_t resulting from an incorrect regressor often causes the real part of $\hat{h}_{0,t}$ to start tracking the imaginary part of $h_{0,t}$ and $Im(\hat{h}_{0,t})$ to track $Re(h_{0,t})$, if the adaptation gain μ is high. This flip in the model tends to prevent the second bit error in the pair from occurring and thus to reduce the BER. The effect is strongest for LMS, which has the highest adaptation gain.

VIII. CONCLUSIONS

In the IS-136 system, LMS adaptation is competitive only in the flat fading case. The WLMS algorithm provides efficient tracking also for two-tap channels. Our results indicate that a single tracking filter designed by underestimating the SIR and overestimating the Doppler speed could offer adequate performance over the entire range of operating conditions. Based on Fig. 10, we conclude that the AR_2 and AR_2I designs provide equal performance in the worst cases, with high disturbance levels and/or fast fading. Due to its simple design, see Theorem 2 in [14], WLMS based on AR_2 modeling becomes the preferred choice, as long as the parameters have zero mean.

The class of WLMS tracking algorithms provides a versatile tool for estimating fast fading channels. Their MSE performance can in the considered case be evaluated theoretically, which reduces the amount of simulation needed in the design of adaptive equalizers.

It should be noted, though, that the predicted steady-state MSE performance neglects initial transient effects. In practice, care must be taken in the initialization of the estimates, so that transient effects do not dominate the actual tracking performance over short data bursts.

It would be of value if tools could also be developed which model and predict the performance loss due to decision errors for adaptive receivers working in decision-directed mode. From simulations, our experience is that the gain μ that minimizes the bit error rate is somewhat higher than the gain that minimizes the MSE tracking performance for known regressors. Another possible generalization is to take information about the regressor uncertainty into account in the tracking design, as suggested in [16].

We have here evaluated the tracking algorithm without utilizing antenna diversity. High-performance channel trackers are, of course, of interest also in conjunction with multi-antenna receivers.

REFERENCES

[1] G. E. Bottomley and K. Molnar, "Adaptive channel estimation for multichannel MLSE receivers," *IEEE Commun. Lett.*, vol. 3, pp. 40–42, 1999.

[2] M.-C. Chiu and C.-C. Chao, "Analysis of LMS-adaptive MLSE equalization on multipath fading channels," *IEEE Trans. Commun.*, vol. 44, pp. 1684–1692, 1996.

[3] L. Davis, I. Collings, and R. Evans, "Coupled estimators for equalization of fast-fading mobile channels," *IEEE Trans. Commun.*, vol. 46, pp. 1262–1265, 1998.

[4] T. Ekman, "Prediction of Mobile Radio Channels," Licentiate, Uppsala Univ., Sweden, 2000.

[5] N. C. Ericsson, S. Falahati, A. Ahlén, and A. Svensson, "Hybrid type-II ARQ/AMS supported by channel predictive scheduling in a multi-user scenario," in *IEEE Vehicular Technology Conf. Fall 2000*, Boston, MA, Sept. 24–28, 2000, pp. 1804–1811.

[6] M. Falkenström, "A Grid Approach to Tracking of Mobile Radio Channels in D-AMPS 1900," Master, Uppsala Univ., Sweden, 1997.

[7] W. C. Jakes, "Multipath interference," in *Microwave Mobile Communications*, W. C. Jakes, Ed.   New York, NY: Wiley, 1974.

[8] K. Jamal, G. Brismark, and B. Gudmundson, "Adaptive MLSE performance on the D-AMPS 1900 channel," *IEEE Trans. Veh. Technol.*, vol. 46, pp. 634–641, Aug. 1997.

[9] S. A. Kassam and V. Poor, "Robust techniques for signal processing: A survey," *Proc. IEEE*, vol. 73, pp. 433–481, 1985.

[10] L. Lindbom, "Simplified Kalman estimation of fading mobile radio channels: High performance at LMS computational load," in *IEEE ICASSP 1993*, vol. 3, Minneapolis, MN, Apr. 27–30, 1993, pp. 352–355.

[11] ——, "A Wiener Filtering Approach to the Design of Tracking Algorithms," Ph.D. dissertation, Dept. Technology, Uppsala Univ., Sweden, 1995.

[12] M. Sternad, L. Lindbom, and A. Ahlén, "Tracking of time-varying systems, Part I: Wiener design of algorithms with time-invariant gains,", www.signal.uu.se/Publications/abstracts/r001.html.

[13] A. Ahlén, L. Lindbom, and M. Sternad, "Tracking of time-varying systems, Part II: analysis of stability and performance of adaptive algorithms with time-invariant gains,", www.signal.uu.se/Publications/abstracts/r002.html.

[14] L. Lindbom, M. Sternad, and A. Ahlén, "Tracking of time-varying mobile radio channels—Part I: The Wiener LMS algorithm," *IEEE Trans. Commun.*, vol. 49, pp. 2207–2217, Dec. 2001.

[15] N. Lo, D. Falconer, and A. Sheikh, "Adaptive equalization and diversity combining for mobile radio using interpolated channel estimates," *IEEE Trans. Veh. Technol.*, vol. 40, pp. 636–645, 1991.

[16] A. Morgul and D. Dzung, "Decision directed channel parameter estimation and tracking using erroneous detectors," *Signal Processing*, vol. 25, pp. 307–318, 1991.

[17] J. Lin, J. G. Proakis, F. Ling, and H. Lev-Ari, "Optimal channel tracking of time-varying channels: A frequency domain approach for known and new algorithms," *IEEE Trans. Select. Areas Commun.*, vol. 13, pp. 141–154, 1995.

[18] J. C. Martin and M. Mintz, "Robust filtering and prediction for linear systems with uncertain dynamics: A game-theoretic approach," *IEEE Trans. Automat. Contr.*, vol. AC-28, pp. 888–896, 1983.

[19] K. J. Molnar and G. E. Bottomley, "Adaptive array processing MLSE receivers for TDMA digital cellular PCS communications," *IEEE J. Select. Areas Commun.*, vol. 16, pp. 1340–1351, 1998.

[20] "PCS IS136-Based Air-Interface Compatibility 1900 MHz Standard, Part I and II,", SP 3388–1, SP 3388–2, J-STD-011.

[21] W. H. Sheen and G. L. Stüber, "MLSE equalization and decoding for multipath fading channels," *IEEE Trans. Commun.*, vol. 39, pp. 1455–1464, 1991.

[22] M. Stojanovic, J. G. Proakis, and J. A. Catipovic, "Analysis of the impact of channel estimation errors on the performance of a decision-feedback equalizer in fading multipath channels," *IEEE Trans. Commun.*, vol. 43, pp. 877–886, 1995.

[23] M. Sternad and A. Ahlén, "Robust filtering and feedforward control based on probabilistic descriptions of model errors," *Automatica*, vol. 29, pp. 661–679, 1993.

[24] M. Sternad, L. Lindbom, and A. Ahlén, "Robust Wiener design of adaptation laws with constant gains," in *IFAC Workshop on Adaptation and Learning in Control and Signal Processing*, Como, Italy, Aug. 2001.

[25] M. K. Tsatsanis, G. B. Giannakis, and G. Zhou, "Estimation and equalization of fading channels with random coefficients," *Signal Processing*, vol. 53, pp. 211–229, 1996.

[26] K. Öhrn, A. Ahlén, and M. Sternad, "A probabilistic approach to multivariable robust filtering and open-loop control," *IEEE Trans. Automat. Contr.*, vol. 40, pp. 405–417, 1995.

Lars Lindbom was born in Västervik, Sweden. He received the M.S. degree in engineering physics and the Ph.D. degree in signal processing from Uppsala University, Uppsala, Sweden, in 1989 and 1998, respectively.

Since 1995, he has been with Ericsson Infotech, Karlstad, Sweden, where he holds a senior specialist position in adaptive filtering for mobile radio systems. His main research interests include adaptive filtering, equalization, and system identification, with applications to wireless communications.

Anders Ahlén (S'80–M'84–SM'90) was born in Kalmar, Sweden. He received the Ph.D. degree in automatic control from Uppsala University, Uppsala, Sweden, in 1986.

From 1984 to 1989, he was with the Systems and Control Group at Uppsala University. From 1984 to 1989, he was an Assistant Professor and, from 1989 to 1992, an Associate Professor. During 1991, he was a Visiting Research Fellow at the Department of Electrical and Computer Engineering, The University of Newcastle, Australia. In 1992, he was appointed Associate Professor in Signal Processing at Uppsala University. Since 1996, he has held the chair in Signal Processing at Uppsala University and is also the head of the Signals and Systems Group at the same university. His research interests, which include signal processing, communications, and control, are currently focused on signal processing for wireless communications.

Prof. Ahlén is the Editor of Demodulation and Equalization for the IEEE TRANSACTIONS ON COMMUNICATIONS.

Mikael Sternad (S'83–M'88–SM'90) received the M.S. degree in engineering physics and the Ph.D. degree in automatic control from the Institute of Technology at Uppsala University, Uppsala, Sweden, in 1981 and 1987, respectively.

He is a Professor in Automatic Control at Uppsala University, Sweden. His main research interest is signal processing applied to mobile radio communication problems, such as long-range channel prediction, used for fast link adaptation and scheduling of packet data flows in wireless mobile systems. He is also involved in acoustic signal processing, in particular compensation of loudspeaker dynamics.

Magnus Falkenström was born in Karlstad, Sweden, on June 25, 1972. He received the M.S. degree in engineering physics from Uppsala University, Uppsala, Sweden, in 1997.

He is currently working at Ericsson Infotech AB, Karlstad, Sweden. His main interest is baseband applications for mobile radio communications, including signal processing and DSP implementation aspects.